Spectrum Map Construction Based on Optimized Sensor Selection and Adaptive Kriging Model

Zhiqing DING [1,2], Jianzhao ZHANG [2], Yongxiang LIU [2], Jie WANG [1], Guokai CHEN [2], Liming CAO [1]

[1] Nanjing University of Information Science and Technology, Nanjing, China
[2] The Sixty-Third Research Institute, National University of Defense Technology, Nanjing, China

20201249259@nuist.edu.cn, jianzhao63s@nudt.edu.cn, lyx63s@163.com, 002915@ nuist.edu.cn
guokai.chen@nudt.edu.cn, 20201249250@nuist.edu.cn

Submitted May 20, 2022 / Accepted July 31, 2022 / Online first August 16, 2022

Abstract. *Spectrum map* (*SM*) *is an important tool to reflect the spectrum usage in the electromagnetic environment. To address the problems of low precision and poor efficiency in the SM construction, this paper develops a novel SM construction approach based on the artificial bee colony enabled sensor layout optimization and an adaptive Kriging model based on spatial autocorrelation. Considering the significant autocorrelation between sensor attributes caused by the exponentially decaying shadow fading of signal propagation, the sensor estimation groups are established, and the estimation results are obtained by the Kriging model. The simulation results show that the proposed SM construction scheme can not only effectively reduce the overhead of sensor resources but also obtain a high SM construction accuracy. Extensive simulation results show that the proposed method can reduce the RMSE of SM construction by 37.56%, 25.32% and 12.89% respectively compared with Random-OK when the standard deviation of shadow fading is 1 dB, 3 dB and 6 dB.*

Keywords

Spectrum map, sensor layout optimization, adaptive Kriging model, spatial autocorrelation, artificial bee colony

1. Introduction

With the rapid development of the 5G era, the Internet of Things, artificial intelligence, Internet of Vehicles, unmanned driving, industrial control, and other fields have ushered in an unprecedented growth trend. In order to cope with the rapidly increasing frequency demand and the increasingly severe "spectrum deficit" [1], cognitive radio [2], [3] technology has been proposed and developed rapidly. The core idea is to perceive and understand the electromagnetic environment, adaptively adjust the working parameters of the radio system, such as frequency, power, modulation type, and coding methods, etc., to adapt to the external wireless environment. The SM visualizes the regional electromagnetic environment by aggregating the usage of the electromagnetic spectrum in a certain area, including the frequency, intensity, location, historical change law and other spectrum data of each signal. It can be used for cognitive radio systems to grasp the occupancy of the surrounding electromagnetic spectrum, to scientifically select available frequencies, and to avoid potential frequency conflicts [4], [5].

The spectrum data required for the SM usually comes from the spectrum sensing networks composed of sensors with radio signal monitoring, receiving and processing capabilities, such as the cognitive communication networks composed of cognitive radio nodes and the specific spectrum monitoring network [6]. Studies have shown that the layout of the sensor nodes in these networks has a great impact on the generation performance of the SM. Due to the limitation of the signal acquisition cost and hardware calculation of radio frequency equipment, the goal of the SM construction is to perform accurate spectrum reconstruction with limited sensors. Karaboga proposed an artificial bee colony (ABC) algorithm to simulate the foraging process of the bee colonies to solve the multi-dimensional multi-peak and valley optimization problem [7]. Therefore, the artificial bee colony algorithm, which has the characteristics of fewer control parameters, simple calculation, and easy implementation, provides a solution for sensor location selection. Due to the non-cooperative nature of radiation sources, it is difficult to obtain accurate prior information on transmitters and propagation models. The performance of current indirect and hybrid methods is highly correlated with the accuracy of prior information and they are therefore not applicable to this problem. Among the direct methods, the Kriging method is a method for spatial modeling and interpolation of random fields and random processes based on covariance functions [8]. It can use the spatial correlation between monitoring data to complete the construction of high-precision SMs [9]. In [10], an adaptive OK interpolation method based on the affinity propa-

DOI: 10.13164/re.2022.0422

gation clustering algorithm (APCA-OK) was proposed to construct the radio environment map (REM) in an efficient manner. The "size of the adaptive estimation group" in [10] was obtained from the experiments of the estimation group based on accuracy and running time, which cannot be adjusted in time in the face of the unknown spectral environment. In [11], an MCS-based REM prototype system was proposed, and ordinary Kriging interpolation was applied to construct a SM. In the process, Kriging interpolation did not make any improvements. The experimental results show that the adaptive Kriging model has better performance. In [12], each decision variable was a given node, and the solution of the node was assumed to be the "path" traversed by ants, which was consistent with the original heuristic ant colony optimization (ACO) framework. The improvement of the ABC proposed in this paper lies in the design of a new perturbation mechanism based on spectral graph construction.

However, SM construction mainly faces two challenges.

Firstly, the relationship between the accuracy of the SM and the sensors location is not clear enough. Most existing work selects sensors by random sampling to return sample data for constructing SMs. For the traditional random sampling layout [13], [14], increasing the number of sensors was the most effective solution for the complex and confrontational application environment. At the same time, it brought the problems of increased data return and calculation overhead, unreliable links, and so on [15]. Marek Suchanski focused on the impact of sensor deployment on the quality of the constructed SMs, and proved through experiments that increasing the number of sensors was beneficial when the number of sensors was small, but continuing to increase the number could not bring significant accuracy improvements [16]. Therefore, if the inherent characteristics of the spatial spectrum situation can be fully exploited, it is possible to construct SMs with less data requirements.

Secondly, the spatial correlation between sensors has not been fully considered in the SM construction process. In [17–19], the spectrum situation of multiple frequency points with multiple time slots was described as an “image”, and an idea of image inference was proposed to construct and to predict the spectrum variation trend. However, these works only dealt with the spectrum data in the time-frequency dimension, without incorporating geographic location, nor considering the correlation between sensors under different signal propagation models. In [20–22], the SMs were constructed by interpolating or mapping known data to unknown points, without considering the correlation between sample attributes caused by the electromagnetic propagation.

In response to the above challenges, this paper uses the artificial bee colony algorithm to select the optimized sensor selection in a limited number of sensors to adaptively construct SMs. The main contributions of this paper are summarized as follows:

- The sensor location selection is optimized using an artificial bee colony algorithm. The optimization process sequentially performs sensor weight processing and selects a new sensor layout with the least fitness of the artificial bee colony. The comparison confirms that the proposed sensor layout optimization selection outperforms random layout selection with less SM error.
- An adaptive Kriging (AK) model SM construction method is proposed. It uses spatial autocorrelation to establish estimation groups of unknown points, and to construct the SMs adaptively, which overcomes the shortage of the weight coefficient allocation in the ordinary Kriging interpolation process. The performance comparison shows that the proposed SM construction scheme has better performance.

The rest of this paper is organized as follows. The second section introduces the scene model of this paper. Section 3 proposes the sensor layout optimization selection based on artificial bee colony algorithm and the SM construction method based on spatial autocorrelation adaptive Kriging model. Section 4 presents the simulation analysis results and the discussion. Finally, a summary is given in Sec. 5.

2. System Model

2.1 Network Architecture

Multiple radiation sources and a set of sensors are arranged in the focused area, where the locations and the transmit powers of the radiation sources are unknown. The sensors measure the received signal strength (RSS) denoted by $P(m_i)$, where m_i is the sensor location. The received signal power of the sensor can be modeled as:

$$P(m_i) = P_{\mathrm{T}} - K - 10\varepsilon \log_{10}(\|m_{\mathrm{p}} - m_i\|) + W_{m_i} \tag{1}$$

where P_{T} is the transmitting power, K is the path loss factor of free space, ε is the path loss exponent, the point m_{p} represents the position of a certain radiation source, $\|\bullet\|$ represents the Euclidean distance between two vectors, and W_{mi} is the shadow loss at the point m_i which obeys the lognormal distribution and satisfies the standard deviation σ [23]. Therefore, the correlation coefficient between point m_i shadow fading W_{m_i} and m_j shadow fading W_{m_j} is [24]:

$$\rho_{i,j} = \frac{E(W_{m_i} W_{m_j})}{\sigma^2} = \exp\left(-\frac{\|m_i - m_j\|}{d_{\mathrm{cor}}} \ln 2 \right) \tag{2}$$

where d_{cor} is the correlation distance when $\rho_{i,j} = 1/\mathrm{e}$ is satisfied [24]. In this case, the shadow correlation coefficient $\rho_{i,j}$ decreases exponentially as the distance between receivers increases.

2.2 Problem Model

The general flow of the SM construction process is shown in Fig. 1. The problem model is divided into three operations: collecting measurements from sensors, selecting sensors, and evaluating field strength or power values at arbitrary locations.

Assume that the given area grid set is $\mathbf{N}$ and the sensors set is $\mathbf{M}$, the subset sensor set $\mathbf{M}^* \subset \mathbf{M}$ is selected as the sensors used to construct the SM. The number of the selected sensors is denoted by $M^* = |\mathbf{M}^*|$. The goal of this paper is to select the optimized set $\mathbf{M}^*$ under the candidate set $\mathbf{M}$ and the positions of each sensor in the area, so as to minimize the error RMSE between the estimated and actual field strength of the constructed SMs. The RMSE is defined by:

$$RMSE = \sqrt{\frac{1}{N}\sum_{i=1}^{N}(\widehat{P}_{n_i} - P_{n_j})^2} \tag{3}$$

where $\hat{P}_{n_i}$ is the estimated RSS of all points in the grid, P_{n_j} is the real value, and N is the total number of grids.

Effective independence method (EFI) is currently one of the most widely used methods in the optimal arrangement of sensors [25]. The core idea of this method is to keep the measurement points that contribute the most to the independence of the target modal vector as much as possible, so as to obtain as much modal information as possible in the case of limited sensors. As an unbiased estimate, the covariance matrix of the estimation error can be given by:

$$\mathbf{P} = E\left[(q-\hat{q})(q-\hat{q})^{\mathrm{T}}\right] = \left[\frac{1}{\sigma^2}\Phi_s^{\mathrm{T}}\Phi_s\right]^{-1} = \mathbf{Q}^{-1} \tag{4}$$

where $\mathbf{Q}$ is the Fisher information matrix. When $\mathbf{Q}$ takes the maximum value, the covariance $\mathbf{P}$ of the estimation error is the smallest, and the generalized modal coordinates can obtain the best unbiased estimation. The Fisher information matrix can be represented as follows:

$$\mathbf{Q} = \frac{1}{\sigma^2}A_0 = \frac{1}{\sigma^2}\Phi^{\mathrm{T}}\mathbf{\Phi} = \frac{1}{\sigma^2}\sum_{i=1}^{n}\Phi_k^{\mathrm{T}}\Phi_k \tag{5}$$

where Φ_k is the mode shape corresponding to the k-th measuring point, that is, the k-th row of $\mathbf{\Phi}$. The vector $\mathbf{E}_D$ for constructing independent distributed states is as follows:

$$\mathbf{E}_D = \mathbf{\Phi\Psi}\lambda^{-1}(\mathbf{\Phi\Psi})^{-1} = \mathbf{\Phi}\left[\Phi^{\mathrm{T}}\mathbf{\Phi}\right]^{-1}\Phi^{\mathrm{T}} \tag{6}$$

where $\mathbf{\Psi}$ is the normalized eigenvector of A_0, λ is the corresponding eigenvalue, and $\mathbf{E}_D$ is an effective independent assignment matrix that characterizes the linearly independent contribution of candidate points to the modal matrix.

According to the idea of independent contribution in EFI, this paper introduces contribution weight coefficient in artificial bee colony, and designs a new perturbation mechanism.

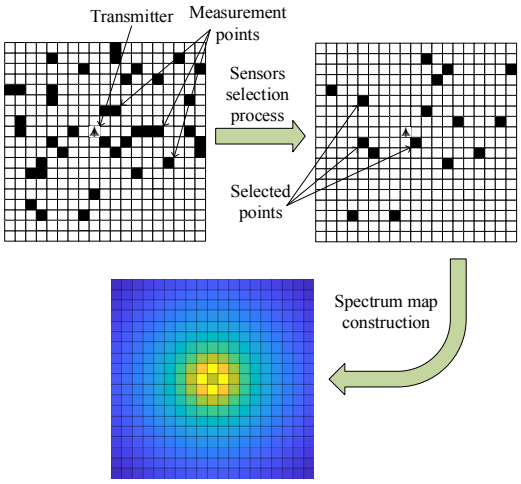

Fig. 1. SM building process.

Then the SM construction problem is modeled as:

$$\mathbf{M}^* = \underset{\mathbf{M}^*\subset\mathbf{M}}{\arg\min}\sum_{i=1}^{N}\left|\widehat{P}_{n_i} - P_{n_j}\right| \tag{7}$$

which is a combinatorial optimization problem, and cannot be addressed within linear time. To this end, this paper proposes a SM construction method that combines the sensor selection and adaptive Kriging model to effectively obtain an approximate optimal solution to problem (7).

3. The Proposed SM Construction Scheme

In this section, SM construction scheme is proposed, including the optimized sensor selection based on artificial bee colony and the construction of SM based on spatial autocorrelation adaptive Kriging model.

3.1 Framework of the Algorithm

ABC-AK generates the optimized sensor selection according to the artificial bee colony, which reduces the cost of sensor resources. Among them, the constraints of the artificial bee colony perturbation mechanism are updated to calculate the weight of each point using the information of the known sensors. Based on the sensor estimation groups established by spatial autocorrelation, unknown points are estimated to improve the accuracy of the SM construction. The flow chart of ABC-AK is shown in Fig. 2, where m^*_i denotes the sensors in the set $\mathbf{M}^*$ and m_i denotes the i-th sensor in the set $\mathbf{M}$.

3.2 Optimized Sensor Selection Based on Artificial Bee Colony

Firstly, we randomly generate initial solutions x_i ($i = 1,2,...NP$) in the search space, in which NP

represents the number of employed bees, and each solution x_i is a D-dimensional vector.

Secondly, the new perturbation mechanism and fitness function is generated. The next state is explored by swapping randomly selected and unselected sensors. The selected sensors are chosen for interpolation, and the unselected sensors are to be interpolated. When selecting a sensor to be replaced, the point that has the least impact on the interpolation accuracy of the current sensor layout is considered here. The number of sensors in the current state is M^*, denoted by $x_1,x_2,\ldots,x_{M^*}$. Then, M^* times interpolation error calculations are used to determine the point in the current layout that has the least impact on the sensor interpolation accuracy. This point will be discarded preferentially by the scout bee as the sensor with the upper limit of exploration in the next state transition. At the same time, when selecting the sensors to be inserted, weight η_i will be considered according to the RMSE of each sensor. The sensor with a larger weight, with a larger RMSE, has a higher probability of being selected, which will speed up the optimized selection of sensor layout. Assuming that the number of sensors of the target is M, M^* sensors are randomly selected as the initial state. Through these M^* sensors, the attribute values of the other $(M-M^*)$ sensors are estimated, and compared with the known values, i.e., the root mean square error RMSE is calculated for the artificial bee colony decision-making. The equation is given by:

$$f = RMSE = \sqrt{\frac{1}{M^*}\sum_{i=1}^{M^*}(\widehat{P_{m_i^*}} - P_{m_j^*})^2} \tag{8}$$

where $\widehat{P_{m_i^*}}$ is the estimated value of the unselected sensor, and $P_{m_i^*}$ is the real data.

Thirdly, the artificial bee colony is improved. The employed bees search for new sensors according to (9), generate a new sensor layout, and share the sensor layout information with onlooker bees, select the sensor layout with the smallest fitness function value according to the greedy strategy to maintain the optimal solution.

$$v_{ij} = u_{i,\text{randsrc}(D,M,\boldsymbol{\eta})} \tag{9}$$

where $i = 1,2,\ldots,NP$, $j = 1,2,\ldots,D$, randscr(·) means randomly choosing D points from M points according to $\boldsymbol{\eta}$, $\boldsymbol{\eta}$ is the weight matrix.

The onlooker bee calculates the selection probability of each sensor according to (10) and selects the sensors with higher weights according to (9) based on the information shared by the employed bee to improve the convergence speed.

$$p_i = \frac{f_i}{\sum_{k=1}^{NP} f_k} \tag{10}$$

where f is the fitness of each solution.

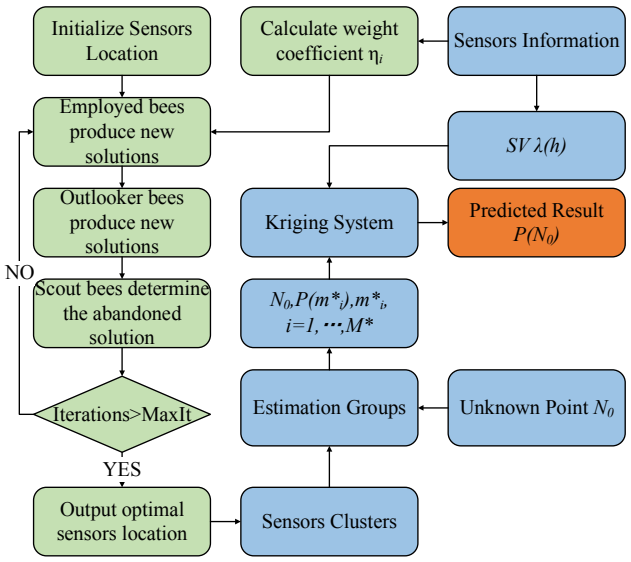

Fig. 2. Flowchart of ABC-AK.

The scout bee discards the sensors that reach the upper limit of exploration and have lower weights according to (11) to find new valuable sensors to enhance the ability to get rid of the local optimum.

$$u_{ij} = u_j^{\min} + r_{ij}\left(u_j^{\max} - u_j^{\min}\right) \tag{11}$$

where r_{ij} is a random number between [0,1].

3.3 SM Construction Based on Spatial Autocorrelation Adaptive Kriging Model

Unknown point estimation often utilizes spatial autocorrelation between sensors to construct SMs. According to the spatial correlation, the sensors are deployed closer to the unknown point, and its measured value has a greater impact on the interpolation result. However, the sensor data is not pre-processed according to the electromagnetic propagation model in the ordinary Kriging model interpolation process. To address this problem, this paper uses spatial autocorrelation to establish sensor estimation groups and proposes an adaptive Kriging model (AK) based on spatial autocorrelation for efficient spectrum recovery. While satisfying the accuracy and efficiency criteria, the key step of AK lies in how to use spatial autocorrelation to find estimated groups from randomly deployed sensors, to select a suitable semivariogram (SV) fitting model, and to obtain estimated values through the Kriging model.

The first step is to find the sensor estimation group. Signals under the propagation model of (1) usually exist in the form of clusters, and the void area is much larger than the spectrum occupied area. So theoretically the spatial autocorrelation of the SM is significant. The most commonly used statistic is Global Moran' I, which is mainly used to describe the average degree of association of all spatial units with surrounding areas in the entire area. The equation is as follows [26]:

$$I = \frac{n}{S_0} \times \frac{\sum_{i=1}^{n}\sum_{j=1}^{n} w_{ij}\left(z_i - \bar{y}\right)\left(z_j - \bar{z}\right)}{\sum_{i=1}^{n}\left(z_i - \bar{z}\right)^2} \quad (12)$$

where I is Moran' I, and its value range is generated randomly between [–1,1]. $I > 0$ means that the attribute values in the target area have a positive correlation in space. $I = 0$ represents a random distribution within the target area, with no spatial correlation. When $I < 0$ indicates that the attribute values in the target area have negative correlations in space. $S_0 = \sum_{i=1}^{n}\sum_{j=1}^{n} w_{ij}$ n is the total number of space units, z_i and z_j represent the attribute values of the i space unit and the j space unit respectively. $\bar{z}$ is the mean value of the attribute values of all space units; w_{ij} represents the spatial weight. The decorrelation distance d_{cor} is defined by the Moran index for the unknown point s_0. As shown in Fig. 3, a set Ω_0 of sensor estimates for point s_0 is established from the decorrelation distance d_{cor}.

The second step is to fit the SV. The SV is the core part of the Kriging model, which quantitatively describes the variable characteristics of the entire region. Equation (13) is defined according to [9].

$$\gamma\left(h\right) = \gamma(d_{ij}) = \frac{1}{2N(d_{ij})}\sum_{i=1}^{N(h)}\left[P\left(s_i\right) - P\left(s_i + d_{ij}\right)\right]^2 \quad (13)$$

where s_i is (x_i,y_i), d_{ij} is the distance between the point (x_i,y_i) and the point (x_j,y_j), and $N(d_{ij})$ is the number of points whose distance is d_{ij}. It selects an appropriate theoretical model to fit an optimal theoretical SV curve, which can more accurately reflect the variation law of variables. The SV conforms to the first law of geography and has similar properties in space [27]. Its theoretical models mainly include the pure gold nugget effect model, spherical model, exponential model, Gaussian model. It has been proved by (2) that the spatial shadow fading coefficient follows an exponential decay, so the fitting of the SV adopts an exponential model and is fitted by least squares:

$$\gamma(h) = C_0 + C\left(1 - \exp\left(-\frac{h}{a}\right)\right) \quad (14)$$

where h is the distance between any two points, C_0 is the nugget constant, $C_0 + C$ is the base value, and a is the step length corresponding to the intersection of the model's tangent at the origin and the base value.

The third step is to establish an adaptive Kriging model. From the sensor samples, the sensor whose distance from the estimated point (x_0,y_0) is less than the decorrelation distance d_{cor} is selected to establish a sensor estimation group Ω_0. It calculates the SV value γ_{ij} between sensors in the estimated group and the SV value between each sensor and the estimated point according to (13). Then, the weight coefficients ω_i are obtained by solving a set of linear equations called the Kriging model by the Lagrange multiplier method, and the linear system is given by:

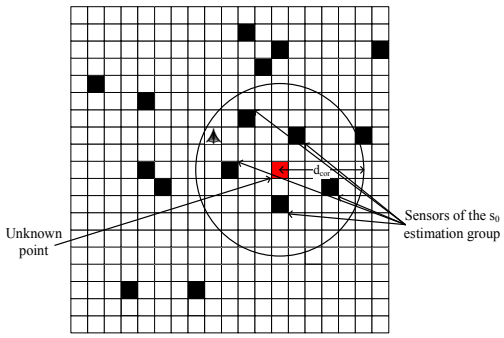

Fig. 3. Estimated set of unknown points.

$$\sum_{i=1}^{n}\omega_i \cdot \gamma_{i0} - \sum_{i=1}^{n}\gamma_{ij} + \phi = 0 \quad (15)$$

where γ_{ij} is the SV value between position (x_i,y_i) and position (x_j,y_j), ϕ is the Lagrange multiplier. The weight coefficient ω_i is the set that can satisfy the minimum difference between the estimated value $\hat{P}_0$ at point (x_0,y_0) and the real value P_0, also satisfies the condition $E\left(\widehat{P_0} - P_0\right) = 0$ for unbiased estimation.

Finally, the estimated point value $\hat{P}_0$ is calculated according to (16)

$$\widehat{P_0} = \sum_{i=1}^{n}\omega_i \cdot P_i \quad (16)$$

where $\hat{P}_0$ is the estimated value (x_0,y_0) of an attribute at point, and P_i is the sample data value.

4. Experimental Results and Discussion

4.1 Setup

In this section, the performance of the proposed SM construction scheme will be evaluated through simulation and real data evaluation. The experiment randomly selects 1000 sensors from all the sensors as known sensors, and selects different numbers of the given available sensors as the input of the experiment to output the sensor layout with the highest accuracy of the spectrum map. In the case of different shadow fading standard deviation, the SM construction performance of different algorithms is analyzed and compared. The parameters' setting is shown in Tab. 1.

The real data experiment adopts the dataset published by Jakob Thrane et al. [28] on IEEE Dataport [29]. The data is real spectrum data measured at 811 MHz and 2630 MHz using Rohde & Schwarz (R&S) TSMW [30], including signal power, signal-to-noise ratio, signal reception strength, etc., and each measurement is synchronized

Parameter	Value
Field dimension	100 × 100 m^2
Signal transmission power (P_T)	30 dBm, 26 dBm, 24 dBm
Signal transmission cartesian coordinates	(20,80), (80,80), (80,20)
Signal frequency	1000 MHz
Path loss factor K	10 dBm
Path loss exponent ε	2
Shadow fading standard deviation (σ)	1 dB, 3 dB, 6 dB

Tab. 1. Propagation model simulation parameter values.

with GPS positioning. The experiment was measured on the campus of the Technical University of Denmark. The mobile spectrum observation device traveled about 14 km and generated about 60,000 data points. All random experiment results in simulation experiments and real data are the average of 500 random experiments. Accuracy is an important criterion for algorithm performance, so the mean square error (RMSE) is used to analyze the accuracy of the RMSE construction, which can be expressed as:

$$RMSE = \sqrt{\frac{1}{l \times w}\sum_{i=1}^{l}\sum_{j=1}^{w}(\hat{P}_{ij} - P_{ij})^2} \tag{17}$$

where l and w are the length and width of the target area, respectively, $\hat{P}_{ij}$ is an interpolation estimate, and P_{ij} is a real value.

4.2 Comparison Based on Simulated Data

Firstly, the performance of the proposed is compared with the counterparts based on the simulation data. As shown in Fig. 4, Fig. 5 and Fig. 6, four different algorithms, including Random-OK, Random-AK, ABC-OK, and ABC-AK SM construction performance, are compared and analyzed based on the different σ of the simulation data. It can be seen that the RMSE of the four algorithms increases with the increase of σ, and ABC-AK performs better than that of the other three algorithms, indicating that ABC-AK has strong robustness. When the numbers of sensors are less than 300, under the same construction method, the sensor-optimized selection performs better than the randomly selected spectrum construction. With same sensor selection method, adaptive Kriging has better SM construction performance than ordinary Kriging.

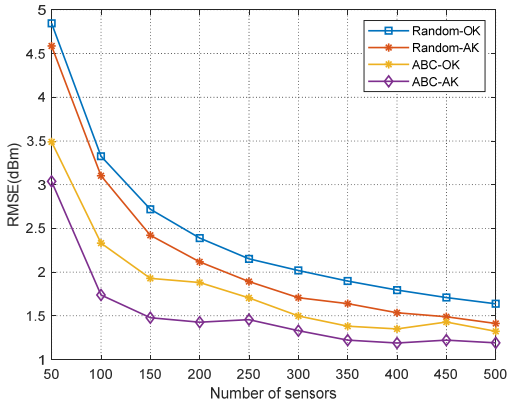

Fig. 4. Performance comparisons for σ = 1 dB.

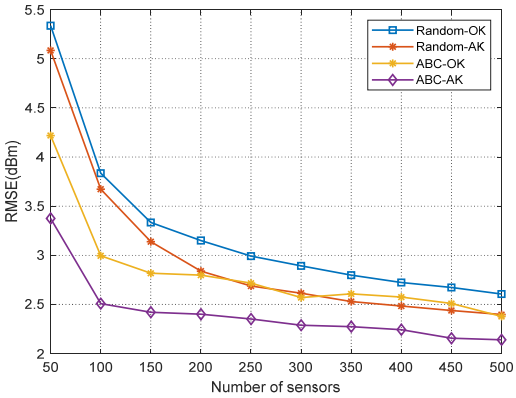

Fig. 5. Performance comparisons for σ = 3 dB.

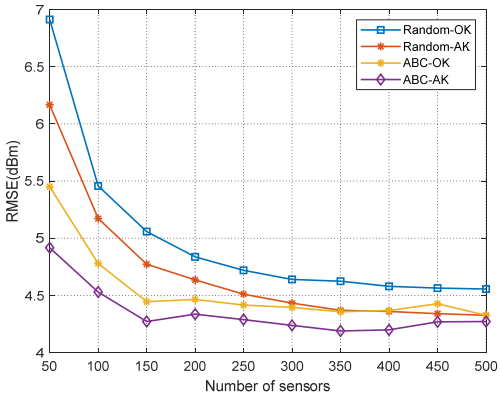

Fig. 6. Performance comparisons for σ = 6 dB.

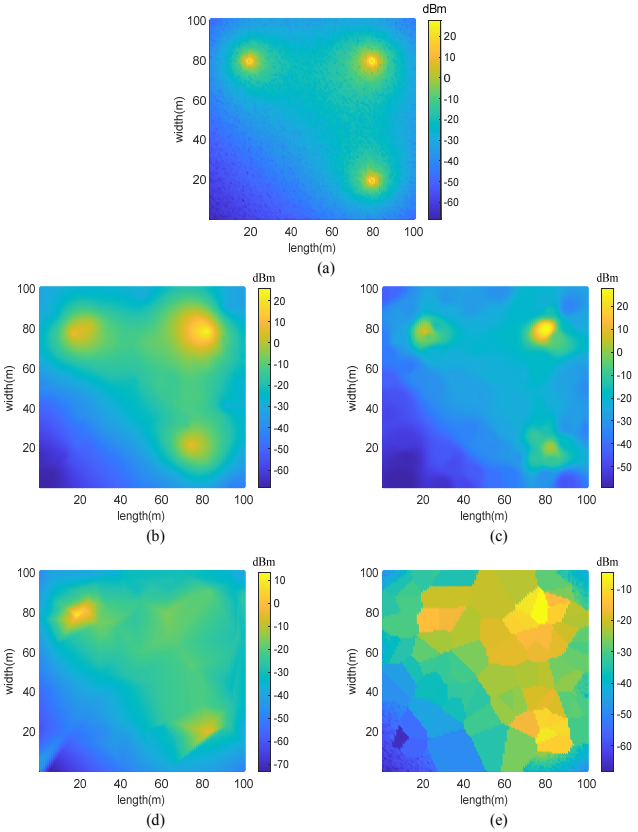

Fig. 7. (a) Original SM of simulation, (b) ABC-SA, (c) Random-IDW, (d) Random-Splines, (e) Random-NN.

When σ is 3 dB and the number of sensors is 100, performance visualizations are made in Fig. 7 to intuitively present the construction performance of the above ABC-SA, Random-IDW, Random-Splines and Random-NN algorithms on localization, source signal strength and SM. It can be found that the ABC-SA algorithm has good performance in all aspects.

4.3 Test Result on Real Data

Secondly, the SM construction of the proposed algorithm is evaluated based on the real measured data. As shown in Fig. 8, based on the measured data, the RMSE of four different algorithms for constructing the SM is compared and analyzed, including Random-OK, Random-AK, ABC-OK, and ABC-AK. It can be seen that the RMSE of all algorithms decreases with the increase of the number of sensors, and ABC-SLO-SA-AK has the best performance in the SM construction. Under the sensor optimization selection, the RMSE of ABC-AK is reduced by 0.30 dBm on average compared with ABC-OK. Under the random selection of sensors, the RMSE of the Random-AK is 0.38 dBm lower than that of the Random-OK. Under ordinary Kriging construction, the RMSE of ABC-OK is 0.71 dBm lower than that of Random-OK on average. Under the adaptive Kriging construction, the RMSE of the ABC-AK algorithm is on average 0.63 dBm lower than that of the Random-AK. In the experiment, the AK algorithm has better performance than the ABC-SLO algorithm. The reason is that AK algorithm adopts an adaptive estimation group, which reduces the influence of low-correlation sensors on the interpolation error and is more conducive to generating the optimized layout.

As shown in Fig. 9, in order to further demonstrate the broad effectiveness of the algorithm, this paper compares different SM construction algorithms based on measured data, including ABC-SA, IDW [31], NN [32], and Splines. It can be seen that the RMSE of each algorithm decreases with the increase of the number of sensors, which indicates that increasing the sample sampling rate is an important factor to improve the accuracy of the SM. Among the four algorithms, the RMSE of the ABC-AK

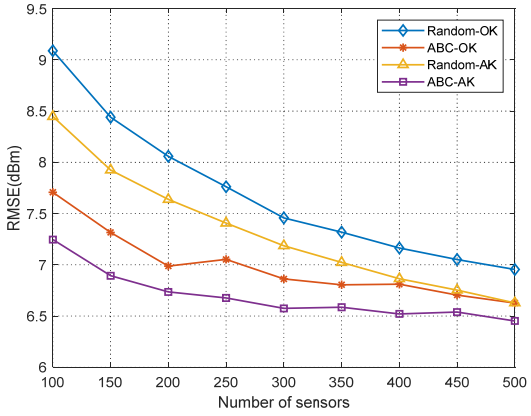

Fig. 8. RMSE comparisons.

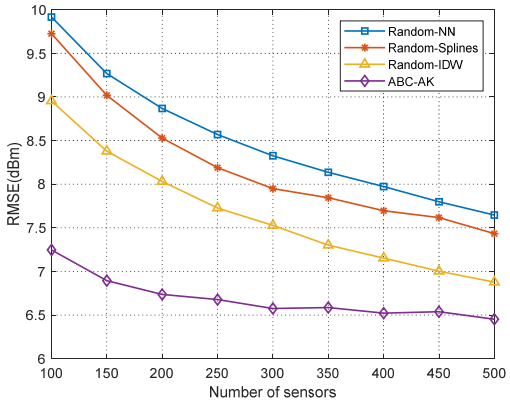

Fig. 9. RMSE based on real measurement data.

algorithm is always smaller than the other three algorithms and is 1.80 dBm, 1.53 dBm, 0.97 dBm lower than the RMSE of the Random-NN, Random-Splines, Random-IDW, respectively. It is proved that the ABC-SLO-SA-AK algorithm has better performance than other algorithms in practice.

5. Conclusion

In this paper, SM construction method based on optimized sensor layout selection and adaptive Kriging model in sensor networks is proposed to achieve high-precision SM construction. The simulation results show that the proposed SM construction scheme can not only effectively reduce the overhead of sensor resources but also obtain a high SM construction accuracy. The analysis based on the measured data shows that ABC-AK provides a feasible solution for the problem of regional SM construction under the condition of sensor sparse. The future work will mainly focus on the construction methods of high-precision SMs for different environments and application constraints.

Acknowledgments

This work was supported by the National Natural Science Foundation of China No. 62131005.

References

[1] MADAN, H. T., BASARKOD P. I. A survey on efficient spectrum utilization for future wireless networks using cognitive radio approach. In *2018 4th International Conference on Applied and Theoretical Computing and Communication Technology* (ICATCCT). Mangalore (India), 2018, p. 47–53. DOI: 10.1109/iCATccT44854.2018.9001951

[2] WANG, B., LIU, K. R. Advances in cognitive radio networks: A survey. *IEEE Journal of Selected Topics in Signal Processing,* 2011, vol. 5, no. 1, p. 5–23. DOI: 10.1109/JSTSP.2010.2093210

[3] CHEN, Y., YU, G., ZHANG, Z., et al. On cognitive radio networks with opportunistic power control strategies in fading

channels. *IEEE Transactions on Wireless Communications,* 2008, vol. 7, no. 7, p. 2752–2761. DOI: 10.1109/TWC.2008.070145

[4] HATTAB, G., IBNKAHLA, M. Multiband spectrum access: Great promises for future cognitive radio networks. *Proceedings of the IEEE,* 2014, vol. 102, no. 3, p. 282–306. DOI: 10.1109/JPROC.2014.2303977

[5] KALATHIL, D. M., JAIN, R. Spectrum sharing through contracts for cognitive radios. *IEEE Transactions on Mobile Computing,* 2013, vol. 12, no. 10, p. 1999–2011. DOI: 10.1109/TMC.2012.171

[6] OGBODO, E. U., DORRELL, D., ABU-MAHFOUZ, A. M. Cognitive radio based sensor network in smart grid: Architectures, applications and communication technologies. *IEEE Access,* 2017, vol. 5, p. 19084–19098. DOI: 10.1109/ACCESS.2017.2749415

[7] KARABOGA, D., AKAY, B. Artificial Bee Colony (ABC) algorithm on training artificial neural networks. In *2007 IEEE 15th Signal Processing and Communications Applications.* Eskisehir (Turkey), 2007, p. 1–4. DOI: 10.1109/SIU.2007.4298679

[8] OLIVER, M. A., WEBSTER, R. A tutorial guide to geostatistics: Computing and modelling variograms and kriging. *CATENA,* 2014, vol. 113, p. 56–69. DOI: 10.1016/j.catena.2013.09.006

[9] SATO, K., INAGE, K., FUJII, T. On the performance of neural network residual Kriging in radio environment mapping. *IEEE Access,* 2019, vol. 7, p. 94557–94568. DOI: 10.1109/ACCESS.2019.2928832

[10] XIA, H., ZHA, S., HUANG, J., et al. Radio environment map construction by adaptive ordinary Kriging algorithm based on affinity propagation clustering. *International Journal of Distributed Sensor Networks,* 2020, vol. 16, no. 5, p. 1–10. DOI: 10.1177/1550147720922484

[11] HAN, Z., LIAO, J., QI, Q., et al. Radio environment map construction by Kriging algorithm based on mobile crowd sensing. *Wireless Communications and Mobile Computing,* 2019, vol. 2019, p. 1–12. DOI: 10.1155/2019/4064201

[12] OKOBIAH, O., MOHANTY, S. P., KOUGIANOS, E. Ordinary Kriging metamodel-assisted ant colony algorithm for fast analog design optimization. In *Thirteenth International Symposium on Quality Electronic Design.* Santa Clara (USA), 2012, p. 458–463. DOI: 10.1109/ISQED.2012.6187533

[13] WANG, Z., LING, C. On the geometric ergodicity of Metropolis-Hastings algorithms for lattice Gaussian sampling. *IEEE Transactions on Information Theory,* 2018, vol. 64, no. 2, p. 738–751. DOI: 10.1109/TIT.2017.2742509

[14] WANG, Z., LING, C. Lattice Gaussian sampling by Markov chain Monte Carlo: Bounded distance decoding and trapdoor sampling. *IEEE Transactions on Information Theory,* 2019, vol. 65, no. 6, p. 3630–3645. DOI: 10.1109/TIT.2019.2901497

[15] FAINT, S., ÜRETEN, O., WILLINK, T. Impact of the number of sensors on the network cost and accuracy of the radio environment map. In *CCECE 2010.* Calgary (Canada), 2010, p. 1–5. DOI: 10.1109/CCECE.2010.5575188

[16] SUCHAŃSKI, M., KANIEWSKI, P., ROMANIK, J., et al. Radio environment maps for military cognitive networks: Density of small-scale sensor network vs. map quality. *EURASIP Journal on Wireless Communications and Networking*, 2020, vol. 2020, no. 1, p. 1–20. DOI: 10.1186/s13638-020-01803-4

[17] TANG, M., DING, G., WU, Q., et al. A joint tensor completion and prediction scheme for multi-dimensional spectrum map construction. *IEEE Access,* 2016, vol. 4, p. 8044–8052. DOI: 10.1109/ACCESS.2016.2627243

[18] SUN, J., WANG, J., DING, G., et al. Long-term spectrum state prediction: An image inference perspective. *IEEE Access,* 2018, vol. 6, p. 43489–43498. DOI: 10.1109/ACCESS.2018.2861798

[19] GE, C., WANG, Z., ZHANG, X. Robust long-term spectrum prediction with missing values and sparse anomalies. *IEEE Access,* 2019, vol. 7, p. 16655–16664. DOI: 10.1109/ACCESS.2018.2889161

[20] KANIEWSKI, P., ROMANIK, J., GOLAN, E., et al. Spectrum awareness for cognitive radios supported by radio environment maps: Zonal approach. *Applied Sciences,* 2021, vol. 11, no. 7, p. 1–23. DOI: 10.3390/app11072910

[21] CHAUDHARI, S., KOSUNEN, M., MAKINEN, S., et al. Spatial interpolation of cyclostationary test statistics in cognitive radio networks: Methods and field measurements. *IEEE Transactions on Vehicular Technology,* 2018, vol. 67, no. 2, p. 1113–1129. DOI: 10.1109/TVT.2017.2717379

[22] SATO, K., SUTO, K., INAGE, K., et al. Space-frequency-interpolated radio map. *IEEE Transactions on Vehicular Technology,* 2021, vol. 70, no. 1, p. 714–725. DOI: 10.1109/TVT.2021.3049894

[23] GUDMUNDSON, M. Correlation model for shadow fading in mobile radio systems. *Electronics Letters,* 1991, vol. 27, no. 23, p. 2145–2146. DOI: 10.1049/el:19911328

[24] HE, R., ZHONG, Z., AI, B., et al. Shadow fading correlation in high-speed railway environments. *IEEE Transactions on Vehicular Technology,* 2015, vol. 64, no. 7, p. 2762–2772. DOI: 10.1109/TVT.2014.2351579

[25] KAMMER, D. C. Sensor placement for on-orbit modal identification and correlation of large space structures. *Journal of Guidance Control and Dynamics,* 1991, vol. 14, no. 2, p. 251–259. DOI: 10.2514/3.20635

[26] CHEN, Y. New approaches for calculating Moran's index of spatial autocorrelation. *PLOS ONE*, 2013, vol. 8, no. 7. DOI: 10.1371/journal.pone.0068336

[27] OLEA, R. A. *Geostatistics for Engineers and Earth Scientists*. US: Springer, 1999. ISBN: 9781461372714

[28] THRANE, J., ZIBAR, D., CHRISTIANSEN, H. L. Model-aided deep learning method for path loss prediction in mobile communication systems at 2.6 GHz. *IEEE Access*, 2020, vol. 8, p. 7925–7936. DOI: 10.1109/ACCESS.2020.2964103

[29] THRANE, J., CHRISTIANSEN, H. L. Mobile communication system measurements and satellite images. *IEEE Dataport,* 2019. DOI: 10.21227/1xf4-eg98

[30] ROHDE-SCHWARZ. *R&S TSMW Universal Radio Network Analyzers User Manual*. 2017. [Online] Available at: https://www.rohde-schwarz.com/uk/manual/r-s-tsmw-universal-radio-network-analyzer-user-manual-manuals-gb1_78701-29128.html

[31] SUCHAŃSKI, M., KANIEWSKI, P., ROMANIK, J., et al. Radio environment map to support frequency allocation in military communications systems. In *2018 Baltic URSI Symposium (URSI).* Poznan (Poland), 2018, p. 230–233. DOI: 10.23919/URSI.2018.8406717

[32] ROMANIK, J., GOLAN, E., ZUBEL, K., et al. Electromagnetic situational awareness of cognitive radios supported by radio environment maps. In *2019 Signal Processing Symposium (SPSympo).* Krakow (Poland), 2019, p. 1–6. DOI: 10.1109/SPS.2019.8882065

About the Authors ...

Zhiqing DING is currently a master student at the School of Electronics and Information Engineering, Nanjing University of Information Technology, Nanjing, China. His research interests include radio map construction methods and wireless communications.

Jianzhao ZHANG received the Ph.D. degree in Communication Engineering from the PLA University of Science and Technology, Nanjing, China, in 2012. He is currently a senior engineer in the Sixty-third Research Institute, National University of Defense Technology, Nanjing, China. His research interests include wireless communications, and dynamic spectrum management.

Yongxiang LIU (corresponding author: The Sixty-Third Research Institute, National University of Defense Technology, Nanjing, China, 210007; E-mail: lyx63s@163.com) received the M.S. degree in Communications and Information Systems from the Institute of Communications Engineering, Nanjing, China, in 1999. He is currently a Professor in the Sixty-third Research Institute, National University of Defense Technology, Nanjing, China. His research interests include wireless communications, spectrum management, and communication anti-jamming.

Jie WANG was born in Jiangsu, China, in 1986. He received the M.Sc. degree in Signal and Information Processing from the University of Chinese Academy of Sciences, Beijing, China, in 2013. He received the Ph.D. degree in Signal and Information Processing from the Science and Technology on Microwave Imaging Laboratory, Institute of Electronics, Chinese Academy of Sciences, University of Chinese Academy of Sciences, Beijing, China, in 2015. Since 2017, he has been with the School of Electronic & Information Engineering, Nanjing University of Information Science & Technology. His research interests include radar waveform designing and processing, joint wireless communication and radar system engineering, and novel radar imaging techniques, such as MIMO and OFDM, and cognitive SAR systems.

Guokai CHEN received a B.S degree in Measurement and Control Technology from the National University of Defense Technology in 2019. He is currently a Ph.D. student in the College of Intelligence Science at the National University of Defense Technology. His research interests include radio map construction methods and radio map-based localization.

Liming CAO is currently a master student at the School of Electronics and Information Engineering, Nanjing University of Information Science and Technology, Nanjing, China. His research interests include wireless sensor network communication and localization based on received signal strength.